Beam Steering mm-Waves Dielectric-only Reflectarray

Andrea Massaccesi
Dept. of Electronics and Telecom.
Politecnico di Torino
Torino, Italy
andrea.massaccesi@polito.it

Michele Beccaria
Dept. of Electronics and Telecom.
Politecnico di Torino
Torino, Italy
michele.beccaria@polito.it

Paola Pirinoli
Dept. of Electronics and Telecom.
Politecnico di Torino
Torino, Italy
paola.pirinoli@polito.it

***Abstract*—In this paper, some numerical results on the possibility to design a 3D-printable dielectric ReflectArray (RA) antenna with beam steering capabilities are presented. The adopted unit-cell consists of a single-layer dielectric element perforated with a square hole, whose side is varied to change the phase of the reflection coefficient. Since the unit-cell behavior is quite stable with the direction of arrival of the incident field, it is used to design a 52×52 reflectarray working in Ka-band. Its numerical characterization proves that the RA is able to provide less than 2 dB of gain losses over a scanning range of $\pm 30^{\circ}$ in the vertical plane.**

***Index Terms*—reflectarray antennas; beam steering; 3D-printed antennas; additive manufacturing.**

I. Introduction

Thanks to their features, ReflectArrays (RAs) [1], [2] have emerged in the last years as successful high-gain antennas characterized by a low profile, reduced complexity and low cost fabrication process, particularly suitable in many applications as satellite communications, radars, point-to-point terrestrial links, remote-sensing systems and deep-space communication links.

In view of their potentialities, many solutions were proposed for the design and realization of reflectarrays; the easiest considered configurations adopted a single patch printed on a dielectric layer as re-radiating element [1], [2], which is however characterized by a narrow bandwidth, and therefore other types of unit-cell, based on the used of elements with more degrees of freedom, printed on different layers, as in [3], [4] or on the same dielectric substrate [5]- [9], were introduced.

Also pushed by the spreading of the use of Additive Manufacturing (AM) techniques for the realization of objects with non conventional shape, recently, new, dielectric-only RA configurations have been introduced. The reflectarrays in [10]- [12] have been designed using dielectric parallelepiped resonators as unit-cells: in [10], [11] the phase of the re-radiated field is controlled through the eight of the unit-cell, while in [12] the dielectric parallelepipeds have a variable transverse section; in all the cases, reduced size RAs have been manufactured using 3D printing techniques. In [13] a C-shaped dielectric unit-cell with heigh approximately equal to 1.5λ at the design frequency of 28 GHz is adopted for the design of a centre fed RA with diameter of 10λ, that can radiate a linear or a circular polarization. Finally, in [14], [15] cross shape elements are introduced to realize dual or circular polarization whose performance have been tested through the manufacturing of small size prototypes.

A feature that antennas for next generation applications must posses is the capability to scan the beam. For what concerns reflectarrays, the most straightforward solution to satisfy this requirement consists in electronically controlling the behaviour of the unit-cell [16], introducing varactors [17], pin diodes [18], MEMS switches [19] or using liquid crystals for its realization [20]. Since the insertion of active components drastically increases the complexity and the cost of the antenna, in some cases an alternative configuration, based on the use of a passive reflective surface can be preferred: in these solutions the 1D or 2D beam-scanning is obtained moving mechanically the feed or using a feed array to change the direction of arrival of the field impinging on the RA surface, with the consequent steering of the beam radiated by the whole antenna [21]- [23]. Despite of its greater simplicity, such an antenna suffers for some degradations of its radiation performance, as the enlargement of the main beam, an increase in the side-lobe level (SLL), a decrease of the maximum gain, and consequently of the efficiency, over the scan range, a narrowing of the bandwidth. To improve the RA features, different techniques have been proposed, as that of designing a bifocal [24] or a multi-focal [25] reflectarray; in [26] the RA is designed to behave as a quasi-spherical reflector, while in [27] the planar reflector is rotated in addition to the feed to cover a larger scan range. Finally, the results summarized in [24], [28] prove that a pseudo-stochastic optimization algorithm can be fruitfully adopted to design a beam scanning reflectarray with enhanced performance.

If the design procedure plays a key role, also the use of a suitable unit-cell, with a proper dependence from the direction of arrival of the incident field, affects the scanning capabilities of a reflectarray. For this reason, the possibility of using the dielectric unit-cell introduced in [29] for the realization of a beam steering RA is here investigated: first the effects of the impinging field incident angle on its behaviour are analyzed, then its use for the design of a medium size reflectarray is considered. The results summarized in Sect.III, obtained through the numerical analysis of a medium sized structure, show its potentials in terms of scan range and bandwidth.

II. Dielectric Unit-Cell

The unit-cell was already introduced in [29], but for sake of clarity its description is summarized in the following, before discussing the influence of the direction of arrival of the incident field on its behavior. As shown in Fig. 1, the unit-cell consists in a dielectric parallelepiped with square basis, backed on a metallic ground plane, and having a square hole in the centre, whose side d is varied to control the phase and the amplitude of the reflection coefficient S_{11}, while its height T is kept constant. Note that the change of hole size corresponds to modify the ratio between the quantity of dielectric material and air in the unit-cell, and therefore to vary its effective dielectric constant.

To make possible the printing of the unit-cell with an AM technique, and in particular with a PolyJet printer, a suitable dielectric material must be used and its geometrical parameters must be optimized to maximize its performance, but also to satisfy the constraints dictated by the tolerances of the manufacturing procedure, as discussed in [30]. In view of these considerations, the chosen material is the 3D-printable resin VeroWhitePlus™ provided by Stratasys® and characterized by $\varepsilon_r = 2.77$ and $\tan\delta = 0.021$. The unit-cell has been designed in Ka-band at the operating frequency $f_0 = 30\,\text{GHz}$. Its optimization has been carried on a frequency interval centred on f_0 and it is organized in three steps, according to which the size W of the unit-cell is first fixed, then the range of variation for the hole size d is determined, taking into account the tolerances of the 3D printing process, and finally T is chosen in such a way to guarantee a range of variation for

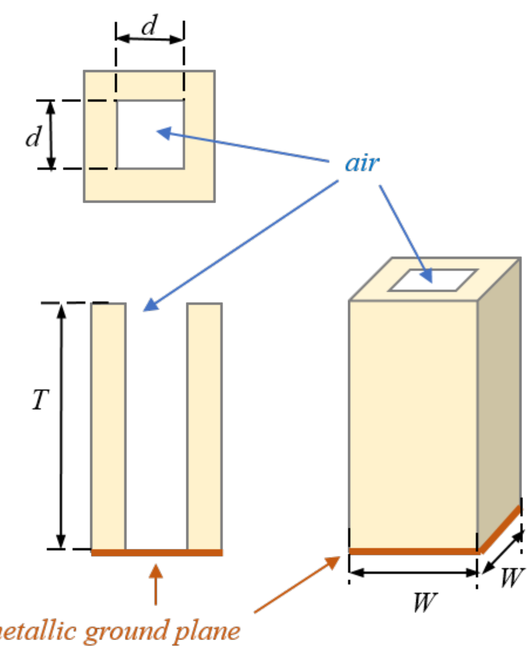

Fig. 1: 3D model of the unit-cell with its side and top views.

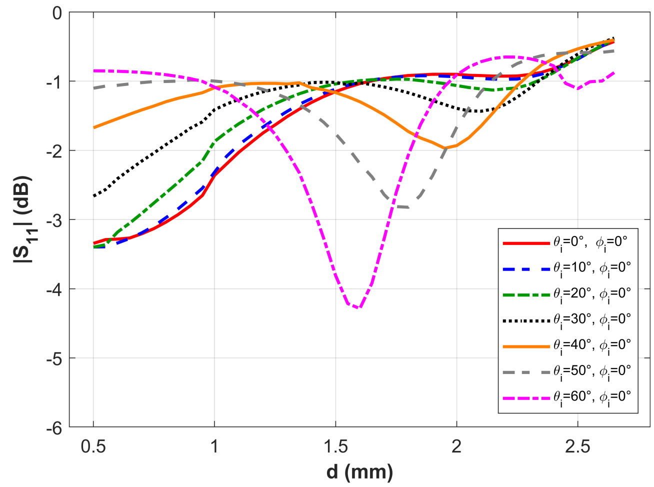

(a)

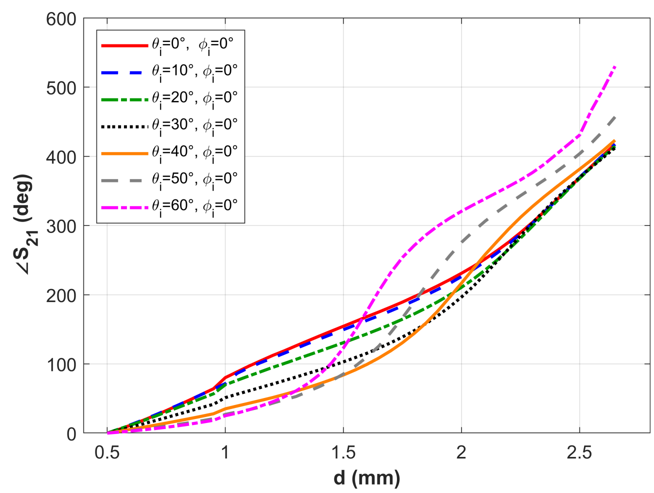

(b)

Fig. 2: Variation of the reflection coefficient S_{11} at 30 GHz with d: a) Amplitude; b) Phase.

the phase of S_{11} of approximately 360°. As the amplitude of this range is directly proportional to ε_r and T, being the relative dielectric constant of the selected material quite low, it is necessary to increase T to obtain the desired phase variation. The resulting values for unit-cell geometrical parameters are the following: $W = 0.3\lambda_0 = 3\,\text{mm}$ and $T = 1.4\lambda_0 = 14\,\text{mm}$, where λ_0 the wavelength evaluated at f_0, while the range of variation for d is fixed to be $[0.5 - 2.65]\,\text{mm}$.

Since the unit-cell would be used for the design of a beam steering RA, its dependence from the direction of arrival of the incident field is studied. In Fig. 2 the variation of the amplitude (top) and phase (bottom) of S_{11} with d evaluated for different values of the incident angles (θ_i, φ_i) is plotted. As can be seen from these results, the greatest limitation on the acceptable value of the incident angle is due to $|S_{11}|$: in fact, while $\angle S_{11}$ does not change significantly till $\theta_i = 50°$, the amplitude of the reflection coefficient decreases in a remarkable way for some values of d when $\theta_i > 30°$. For lower values, the influence of the direction of arrival of the incident field is negligible, and this confirms the possibility to use the considered unit-cell for the design of a beam steering reflectarray.

III. Beam Steering Reflectarray

The unit-cell described above is adopted for the design of a squared reflectarray with side $D = 15.6\lambda_0$, discretized with 2704 unit-cells. The beam is steered moving the feed along a circular arc, whose radius F, defined as the distance between the feed and the centre of the planar surface, is such that $F/D = 1$. The distribution of $\angle S_{11}$ provided by the RA surface is shown in Fig.3.

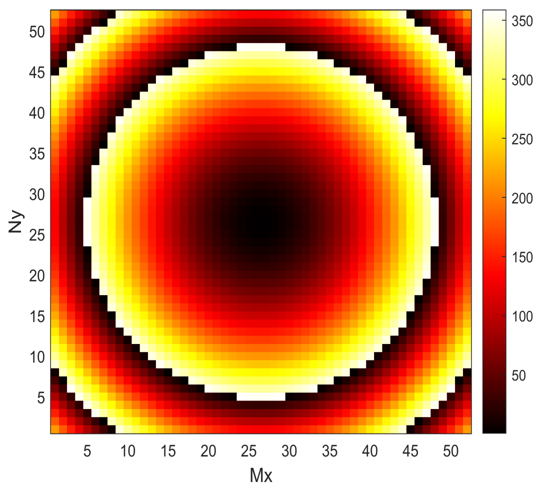

Fig. 3: Required phase distribution the of 52×52 dielectric perforated RA.

The reflectarray has been numerically analyzed with CST Microwave Studio: the resulting radiation patterns in the E- (top) end H- (bottom) planes are shown in Fig. 4, for different values of θ_i, that correspond to different directions of maximum radiation. As it appears from these plots, in both the planes the radiation patterns are slightly affected by the beam steering over the considered interval ranging from -30° to +30° in the E-plane. For $\theta_i = \pm 10°$ and $\theta_i = \pm 20°$ the main beam stays almost the same both in the E- and in the H-plane, while it suffers for a contained reduction and enlargement when $\theta_i = \pm 30°$.

It is worth to notice that generally a given variation of the incident angle does not correspond to the same change in the direction of maximum radiation, but the two quantities are related by the Beam Deviation Factor (BDF) defined as the ratio between the direction of maximum radiation and the incident angle. In case of beam scanning configurations, the BDF can be not the same for all the pointing directions, and therefore it becomes more complex to fix the position of the feed, from which (θ_i, φ_i) depend, for obtaining the desired pointing direction; in the present case this problem does not subsist, since BDF $= 0.9$ over the entire scanning range.

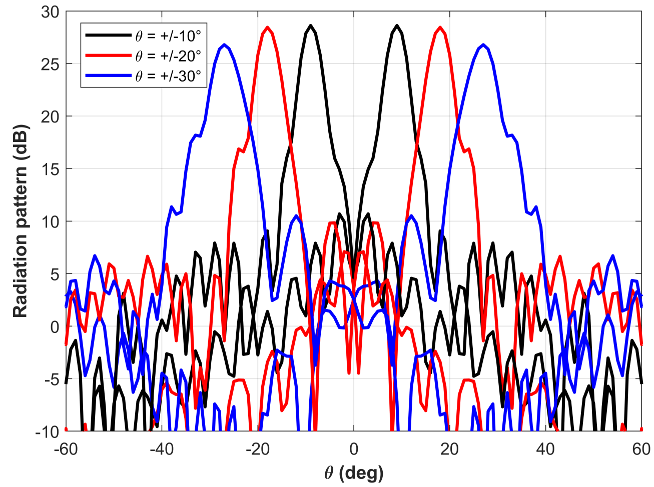

(a)

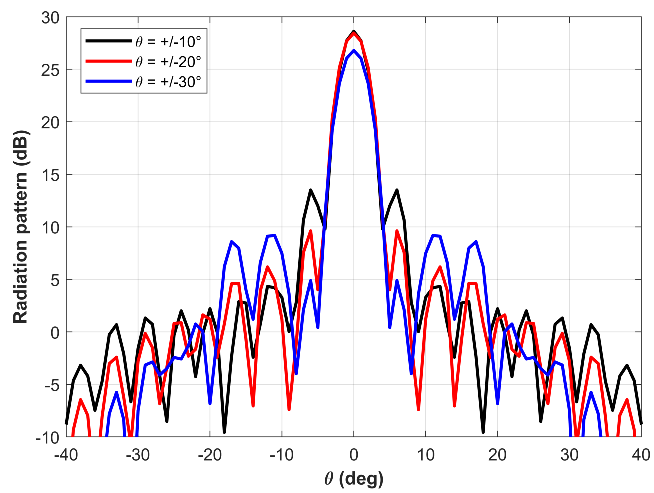

(b)

Fig. 4: Radiation patterns of the designed reflectarray for different directions of maximum radiation in the E-plane (a) and H-plane (b).

A summary of the radiation performance of the reflectarray for θ_i equal to $\pm 10°$, $\pm 20°$ and $\pm 30°$ is finally reported in Table I. The values of the maximum gain listed in the first row confirm that the use of the dielectric unit-cell provides scan

TABLE I: Summary of the RA performance for different pointing directions

θ_i	$\pm 10°$	$\pm 20°$	$\pm 30°$
max gain	28.6 dBi	28.65 dBi	26.8 dBi
1-dB bandwidth	11.3 %	10.9 %	10.1 %
$HPBW_E$	4.0°	4.3°	5.5°
$HPBW_H$	3.5°	3.8°	3.9°
SLL (E-plane)	-17.9 dB	-11.6 dB	-8.6 dB
SLL (H-plane)	-15.1 dB	-18.8 dB	-21.2 dB

losses over the considered range no larger than 1.8 dB, while the main beam has an almost constant width in the H-plane (row 4) and an enlargement of approximately 1.5° in the E-plane (row 3), where the beam steering occurs. Noticeable is the result about the 1-dB bandwidth, that is wider than 10% over the entire scanning range, i.e. very close to the value obtained in the case of the fixed beam RA in [29] and this confirms the good performance of the unit-cell.

IV. CONCLUSIONS

In this paper, a dielectric unit-cell is used to design a reflectarray with good beam steering capabilities: this is due essentially to the reduced dependence of the unit-cell behavior from the direction of arrival of the incident field. Moreover, its broadband attitude guarantees that the radiation performance of the RA stays stable not only over a significative scanning range but also over a frequency band larger than 10%, as proved by the reported numerical results.

REFERENCES

[1] J. Huang and J. Encinar, Reflectarray antennas. Wiley-IEEE press, 2008.

[2] P. Nayeri, F. Yang, and A. Z. Esherbeni, Reflectarray antennas: theory, designs and applications, Hoboken, NJ, USA: Wiley, 2018.

[3] J.A. Encinar, “Design of two-layer printed reflectarray using patches of variable size,” IEEE Trans. Antennas Propag., vol. 49, no. 10, pp. 1403-1410, Oct. 2001

[4] J.A. Encinar and J.A.Zornoza, “Broadband design of three-layer printed reflectarrays,” IEEE Trans. Antennas Propag., vol. 51, no. 7, pp. 1662-1664, July 2003.

[5] M.R. Chaharmir, J. Shaker and H. Legay, “Broadband design of a single layer large reflectarray using multi cross loop elements,” IEEE Trans. Antennas Propag., vol. 57, no. 10, 3363-3366, Sept. 2009.

[6] J.H. Yoon, Y.J. Yoon, W.-S. Lee and J.-H. So , “Broadband microstrip reflectarray with five parallel dipole elements,” IEEE Antennas Wireless Propag. Lett., vol. 14, pp. 1109-1112, Jan. 2015.

[7] Q. Wang, Z.H. Shao, Y.J. Cheng, P.K. Li, “Broadband low-cost reflectarray using modified double-square loop loaded by spiral stubs,” IEEE Trans. Antennas Propag., vol. 63, no. 9, pp. 4224-4229, June 2015.

[8] X. Li, X. Li, Y. Luo, G. Wei and X. Yi, “A Novel Single Layer Wideband Reflectarray Design Using Two Degrees of Freedom Elements,” IEEE Trans. Antennas Propag., vol. 69, no. 8, pp. 5095-5099, Aug. 2021.

[9] D. Kundu, D. Bhattacharya and R. Ruchi, “A Single-Layer Broadband Reflectarray in K-Band Using Cross-Loop Slotted Patch Elements,” in IEEE Access, vol. 10, pp. 13490-13495, 2022.

[10] S. Zhang, “Three-dimensional printed millimetre wave dielectric resonator reflectarray,” IET Microw. Antennas Propag., vol. 11, no. 14, pp. 2005-2009, 2017.

[11] M.D. Wu et al., “Design and Measurement of a 220 GHz Wideband 3-D Printed Dielectric Reflectarray,” IEEE Antennas Wireless Propag. Lett., vol. 17, no. 11, pp. 2094-2098, Nov. 2018.

[12] E.-C. Choi and S. Nam, “High-Efficiency Dielectric Reflectarray Antennas With Ultra-Wideband Characteristics,” IEEE Access, vol. 9, pp. 152075-152081, 2021.

[13] P. Mei, S. Zhang and G. F. Pedersen, “A Wideband 3-D Printed Reflectarray Antenna With Mechanically Reconfigurable Polarization,” IEEE Antennas Wireless Propag. Lett., vol. 19, no. 10, pp. 1798-1802, Oct. 2020.

[14] B. Li, C. Y. Mei, Y. Zhou and X. Lv, “A 3-D-Printed Wideband Circularly Polarized Dielectric Reflectarray of Cross-Shaped Element,” IEEE Antennas Wireless Propag. Lett., vol. 19, no. 10, pp. 1734-1738, Oct. 2020.

[15] Y.-X. Sun, D. Wu and J. Ren, “Millimeter-Wave Dual-Polarized Dielectric Resonator Reflectarray Fabricated by 3D Printing With High Relative Permittivity Material,” IEEE Access, vol. 9, pp. 103795-103803, 2021.

[16] S.V. Hum and J. Perruisseau-Carrier, “Reconfigurable reflectarrays and array lenses for dynamic antenna beam control: a review,” IEEE Trans. Antennas Propag., vol. 62, no. 1, pp. 183-198, 2014.

[17] L. Boccia, G. Amendola, and G. Di Massa, “Performance improvement for a varactor-loaded reflectarray element,” IEEE Trans. Antennas Propag., vol. 58, no. 2, pp. 585-589, 2010.

[18] H. Yang, et al., “A 1-bit 10×10 reconfigurable reflectarray antenna: Design, optimization, and experiment,” IEEE Trans. Antennas Propag., vol. 64, no. 6, pp. 2246-2254, Jun. 2016.

[19] T. Debogovic and J. Perruisseau-Carrier, “Low-loss MEMS-reconfigurable 1-bit reflectarray cell with dual-linear polarization,” IEEE Trans. Antennas Propag., vol. 62, no. 10, pp. 5055-5060, Oct. 2014.

[20] X. Meng, M. Nekovee and D. Wu, “The Design and Analysis of Electronically Reconfigurable Liquid Crystal-Based Reflectarray Metasurface for 6G Beamforming, Beamsteering, and Beamsplitting,” IEEE Access, vol. 9, pp. 155564-155575, 2021.

[21] P. Nayeri, F. Yang, and A. Z. Elsherbeni, “Beam-Scanning Reflectarray Antennas: A Technical Overview and State of the Art,” IEEE Antennas Propag. Mag., vol. 57, no. 4, pp. 32-47, Aug. 2015.

[22] G.-B. Wu, S.-W. Qu, and S. Yang, “Wide-Angle Beam-Scanning Reflectarray With Mechanical Steering,” IEEE Trans. Antennas Propag., vol. 66, no.1, pp. 172-181, Jan. 2018.

[23] P. Mei, S. Zhang, and G. F. Pedersen, “A Low-Cost, High-Efficiency and Full-Metal Reflectarray Antenna With Mechanically 2-D Beam-Steerable Capabilities for 5G Applications,” IEEE Trans. Antennas Propag., vol. 68, no. 10, pp. 6997-7006, Oct. 2020.

[24] P. Nayeri, F. Yang and A. Z. Elsherbeni, “Bifocal Design and Aperture Phase Optimizations of Reflectarray Antennas for Wide-Angle Beam Scanning Performance,?” IEEE Trans. Antennas Propag., vol. 61, no. 9, pp. 4588-4597, Sept. 2013.

[25] P. Pirinoli, T. Lohrey, M. Orefice, M. Beccaria and G. Dassano, “Multifocal Approach for Reflectarray Antenna for DTH Applications,” 15th Eur. Conf. on Antennas Propag. (EuCAP), Dusseldorf, Germany, 2021, pp. 1-4.

[26] P. Pirinoli, T. Lohrey, M. Orefice, M. Beccaria and G. Dassano, “Reflectarray with mechanically steerable beam for DTH application,” 49th Eur. Microw. Conf. (EuMC), Paris, France, 2019, pp. 141-144.

[27] G.-B. Wu, S. -W. Qu, S. Yang and C. H. Chan, “Low-Cost 1-D Beam-Steering Reflectarray With ±70° Scan Coverage,” IEEE Trans. Antennas Propag., vol. 68, no. 6, pp. 5009-5014, June 2020.

[28] A. Niccolai, M. Beccaria, R. E. Zich, A. Massaccesi and P. Pirinoli, “Social Network Optimization Based Procedure for Beam-Scanning Reflectarray Antenna Design,” IEEE Open J. of Antennas Propag., vol. 1, pp. 500-512, 2020.

[29] A. Massaccesi, M. Beccaria and P. Pirinoli, “3D-printable Perforated Dielectric Reflectarray in Ka-band,” 2019 IEEE Int. Symp. on Antennas Propag. , Atlanta, GA, USA, 2019, pp. 295-296.

[30] A. Massaccesi, et al., “3D-Printable dielectric transmitarray with enhanced bandiwidth at millimiter-waves,” IEEE Access, vol. 6, pp. 46407-46418, 2018.